Multistep Direct Mechanism in the ($\vec{p}$,^{3}He) Inclusive Reaction on ^{59}Co and ^{93}Nb at Incident Energies between 100 and 160 MeV

A. A. Cowley[1,2], J. Bezuidenhout[1], S. S. Dimitrova[3], P. E. Hodgson[4],
S. V. Förtsch[2], G. C. Hillhouse[1], N. M. Jacobs[1], R. Neveling[2], F. D. Smit[2],
J. A. Stander[1], G. F. Steyn[2], and J. J. van Zyl[1]

[1] Department of Physics, University of Stellenbosch, Private Bag X1, Matieland 7602, South Africa
[2] iThemba Laboratory for Accelerator Based Sciences, PO Box 722, Somerset West 7129, South Africa
[3] Institute for Nuclear Research and Nuclear Energy, Bulgarian Academy of Sciences, 1784 Sofia, Bulgaria
[4] Nuclear Physics Laboratory, Department of Physics, University of Oxford, Oxford OX1 3RH, United Kingdom

Abstract. Inclusive ($\vec{p}$,^{3}He) reactions on ^{59}Co and ^{93}Nb were investigated at incident energies of 130 and 160 MeV. Emission-energy distributions for cross sections as well as analyzing powers were measured from a threshold of $\backsim$ 40 MeV up to the kinematic maximum. An angular range from 15° to 140° (lab.) was covered. The experimental distributions are compared with a multistep direct theory in which a reaction mechanism based on deuteron pick-up is employed. Reasonable agreement between experimental double differential cross sections and analyzing powers and the theoretical expectation is obtained. This work, together with published results for the same reaction and targets at a lower projectile energy of 100 MeV, allows the incident-energy dependence to be explored.

1 Introduction

During the last few years there have been many studies of reactions of high energy protons with nuclei in which the final states are not resolved. The simplest are the (p,p') and (p,n) reactions followed by the (p,d) reaction. The next in order of increasing complexity are the (p,^{3}He) and (p,α) reactions. These reactions are of interest for several reasons; firstly it is interesting to see which among the possible reaction mechanisms contribute and what the relative strengths of their contributions are. Secondly it is interesting to see what features of nuclear structure can be revealed by analyzing the reactions. The present work concentrates on the (p,^{3}He) reaction, but it is useful for the purposes of comparison to begin by making a few remarks about the existing analyses of the (p,α) reaction.

The (p,α) reaction can take place by two principal mechanisms, namely by the pickup of a triton or by the knockout of an α-particle. These mechanisms can be distinguished in principle by calculating the cross sections and analyzing powers expected from each mechanism and comparing with the experimental data. It is found, however, that the results of such calculations for reactions to discrete final states are so similar that they do not permit the identification of the mechanism taking place. However nuclear structure arguments indicate that the pickup mechanism dominates. In the case of reactions to the continuum the differential cross sections corresponding to the two mechanisms are very similar, but the calculated analyzing powers are very different [1]. Comparison with the data for the reaction on ^{58}Ni at an incident energy of 72 MeV shows that the dominant mechanism is knockout, and this is also reasonable on dynamical grounds. The (p,α) reaction is also useful to excite and study the α-particle states of nuclei. It is notable that these calculations have been made treating the triton and the α-particle as a cluster, and the success of this relatively crude approximation indicates that it would be difficult to obtain additional information by analyzing these reactions in a more complicated way in which the nucleons are treated as separate constituents.

In this paper we present new results for the inclusive ($\vec{p}$,^{3}He) reaction on ^{59}Co and ^{93}Nb at incident energies of 130 and 160 MeV, and emission-energy distributions are measured for cross sections as well as analyzing powers. The choice of incident energy is determined by existing analyzing power results for the inclusive ($\vec{p}$,^{3}He) reaction that are available at 100 MeV [2] and also at 200 MeV [3]. Based on the results at these two incident energies, the expectation is that the analyzing powers should become negligible as the incident energy approaches 200 MeV, thus favoring a much lower incident energy for reasonably rapid collection of data with good statistical accuracy. The two target nuclei were selected because they are naturally isotopically pure and they are assumed to be representative examples of target species.

The experimental procedure is described in Section 2. The experimental distributions are analyzed in terms of a multistep direct theory that assumes a deuteron pick-up reaction mechanism, as detailed in Section 3. In Section 4 the results are presented, and Section 5 contains a summary and conclusion.

2 Experimental Procedure

The cross sections and analyzing powers were measured at iThemba Laboratory for Accelerator Based Sciences, Faure, South Africa. The accelerator and the experimental equipment have been described elsewhere [4]. The details of the present measurements of cross section and analyzing power distributions for the inclusive ($\vec{p}$,^{3}He) reactions on ^{59}Co and ^{93}Nb at incident energies of 130 and 160 (± 0.5) MeV are very similar to those described in our earlier work [2] at 100 MeV, and some salient features are repeated here.

The projectile protons were polarized to approximately 80%. In order to reduce systematic errors on the analyzing power measurements, the polarization of the incident beam was switched from up to down at 5 second intervals. The difference in the polarization between the two orientations was always less than 8%.

Two detector telescopes, each consisting of a 500 μm silicon surface barrier detector followed by a NaI(Tℓ) crystal connected to a photomultiplier tube, were used. Particle identification was achieved with a standard ΔE–E technique. This allowed the reliable separation of the ^{3}He particles of interest from other ejectiles, especially α particles.

The two detector telescopes were collimated to the same nominal solid angle acceptance by means of Ta collimators, and used at symmetric scattering angles on opposite sides of the beam. This arrangement, together with the switching of the polarization state, is the standard method of minimizing the systematic error of the analyzing power measurement.

Energy calibrations of the silicon surface barrier detectors were made using a ^{228}Th α-particle source, and the calibrations of the NaI(Tℓ) detector elements were based on the kinematics of the elastic scattering reactions ^{1}H$(p,p)^1$H and ^{12}C$(p,p)^{12}$C from a thin polyethylene target. These calibrations for protons in the telescope also provide energy values for ^{3}He, if the difference in the response of these ejectiles with the NaI(Tℓ)-assembly is taken into account [5]. Gain drifts in the photomultiplier tubes of the NaI detectors were monitored by a light-emitting diode pulser system which allowed corrections to be made during analysis. These procedures lead to a 4% uncertainty in the energy scale for ^{3}He.

The self–supporting targets were metals of natural elements (100% occurrence of the isotope of interest) with thicknesses in the range of 1 to 5 mg/cm^2. The uncertainty in the thicknesses of the targets (up to 8%) is the main contribution to the systematic error on the cross section data.

3 Theoretical Analysis

The ($\vec{p}$,^{3}He) double differential cross section and analyzing powers were calculated using a formulation based on the multistep direct theory of Feshbach, Kerman and Koonin (FKK) [6]. Bonetti *et al.* [7] describe the extension of the FKK theory to obtain a formulation of the analyzing power.

(i) Calculation of differential cross sections

The double differential cross section may be expressed as

$$\frac{d^2\sigma}{d\Omega dE} = \left(\frac{d^2\sigma}{d\Omega dE}\right)^{\text{one-step}} + \left(\frac{d^2\sigma}{d\Omega dE}\right)^{\text{two-step}} + \dots \,, \tag{1}$$

where the first step cross section is taken as a direct two-nucleon $(p,^3$ He) process calculated in terms of the DWBA for a reaction into the continuum of excitation. Therefore

$$\left(\frac{d^2\sigma}{d\Omega dE}\right)^{\text{one-step}} = \sum_{N,L,J} \frac{(2J+1)}{\Delta E}\frac{d\sigma^{DW}}{d\Omega}(\theta, N, L, J, E) \,, \tag{2}$$

where the summation runs over the target states with single–particle energies within a small interval $(E - \Delta E/2, E + \Delta E/2)$ around the excitation energy E. The last factor in Eq. 2 is the DWBA differential cross section which is given by [8, 9]:

$$\frac{d\sigma^{DW}}{d\Omega}(\theta, N, L, J, E) = \mathcal{N} \sum_{\{n_k\}} G^2(\{n_k\}^2) \frac{2J_f + 1}{2J_i + 1} \sum_{T=0,1} b_{ST}^2 D_{ST}^2 \times \langle T_f T_{fz} T T_z | T_i T_{iz} \rangle^2 \left(\frac{d\sigma}{d\Omega} \right)^{\mathrm{DWUCK}}, \quad (3)$$

where the sum runs over all possible neutron–proton configurations $\{n_k\}$. Here $\mathcal{N}$ is a normalization constant whose value depends on the square of the fractional parentage coefficient for the two–nucleon removal [10] as well as the optical model potentials. The quantity $G^2(\{n_k\}^2)$ is the spectroscopic factor for a proton and neutron to form a deuteron bound state with quantum numbers (N, L, J), and S and T are the transferred spin and isospin, respectively, with the selection rule $S + T = 1$. Because the microscopic calculation of the pickup of a neutron-proton pair gives essentially the same result as a macroscopic calculation in which the nucleon pair is treated as a deuteron cluster [9], we approximate the target nucleus as consisting of a core to which a deuteron is bound in a shell–model state. The $(p,^3\mathrm{He})$ reaction can then be described as a direct transition of a deuteron, considered as a single particle. Final and initial total angular momenta are indicated by J_f and J_i, respectively.

The quantity b_{ST}^2 is 0.5 for both values of S and T, and the values for the strengths of the proton–deuteron interaction D_{10}^2 and D_{01}^2 are 0.3 and 0.72 respectively [11]. The square of the Clebsch–Gordan coefficient depends on initial, transferred and final isospins T_i, T, and T_f .

The differential cross sections $\left(\frac{d\sigma}{d\Omega} \right)^{\mathrm{DWUCK}}$ to particular (N, L, J, T) states are calculated using the code DWUCK4 [12].

The form factor of the deuteron is obtained by the usual procedure of adjusting the well depth of a Woods–Saxon potential with geometrical parameters $r_0 = 1.15$ fm and $a = 0.76$ fm [13, 14] to obtain the correct binding energy and wave function characteristics . This results in microscopic and macroscopic form factors that are almost identical.

The global optical potentials of Madland-Schwandt [15, 16] for protons are used. In previous work [17] it was found that the calculated cross sections were rather insensitive to the potential of the incident proton, but very sensitive to the specific potential set adopted for ^{3}He. For consistency, therefore, as in [2] we used a microscopic optical potential for ^{3}He obtained by the double folding model [18, 19] defined by:

$$V_{DF}(\mathbf{R}) = \int d\mathbf{r}_1 d\mathbf{r}_2 \; \rho_{^3\mathrm{He}}(\mathbf{r}_1) \; \rho_A(\mathbf{r}_2) \; v_{eff}(\mathbf{r}_1 + \mathbf{R} - \mathbf{r}_2) \, , \quad (4)$$

where $\rho_{^3\mathrm{He}}(\mathbf{r}_1)$ and $\rho_A(\mathbf{r}_2)$ are the local density of ^{3}He and the target nucleus A respectively, and $v_{\mathrm{eff}}(\mathbf{r}_1 + \mathbf{R} - \mathbf{r}_2)$ is an effective nucleon-nucleon interaction. In the present calculations we use the DDM3Y effective nucleon-nucleon interaction originally introduced by Kobos *et al.* [20]. The code MOPHE3 of Katsuma and Sakuragi [21] was used to calculate this double folding potential. It should be noted that the DDM3Y effective interaction is real and it has a weak energy-dependence.

For the imaginary part of the optical potential a volume Woods-Saxon form is added and the parameters are adjusted to give a reasonable reproduction of the cross section and analyzing power at a high emission energy where the first step reaction dominates. The way in which the parameters of this imaginary potential is determined does not allow its energy dependence to be extracted with any degree of confidence, but we nevertheless find a need to use values which vary systematically as a function of incident proton energy. This suggests that our adoption of an energy-independent imaginary potential for the emitted ^{3}He at each respective energy value of the incident proton is a rather crude approximation.

The final double folding potential $V_{DF}(\mathbf{R})$ thus has the form:

$$V_{DF}(\mathbf{R}) = U_C^{DF}(\mathbf{R}) + U_{SO}^{DF}(\mathbf{R})\mathbf{L}.\mathbf{S} + iW^{WS}(\mathbf{R}) \ , \tag{5}$$

where $U_C^{DF}(\mathbf{R})$ and $U_{SO}^{DF}(\mathbf{R})$ are the central and the spin-orbit parts of the double folding potential respectively, and $W^{WS}(\mathbf{R})$ is the phenomenological imaginary part of the potential. For reasons which are spelled out by various authors (see for example [18]) one should allow for renormalisations of the central as well as the spin-orbit parts of the folded potential.

The convolution structure of the formalism allows the calculation of multistep processes, in particular the two–step $(p, p',^3\text{He})$ and three–step $(p, p', p'',^3\text{He})$ reactions. The $(p, n,^3\text{He})$ reaction was not included because it requires the pick–up of a di–proton. The (p, p') and (p, p', p'') double differential cross sections which are needed for calculating the contributions of the second- and third-step processes were taken from [22]. These distributions originate from the FKK multistep direct reaction theory which describe inclusive $(p, p^{'})$ cross section distributions [23] on target nuclei which are close to those needed for this work and which cover the same incident energies as in the present investigation.

Because the deuteron formation probability is not known, the theoretical differential cross sections at each incident energy were normalised independently to the experimental data at a high outgoing energy where the first step dominates. No further normalisation was allowed at different emission energies. The analyzing power distributions are not affected by this procedure as they are calculated from ratios of cross sections.

(ii) Calculation of the analyzing power

The analyzing power in terms of protons fully polarised in the positive (up) direction as defined by the Basel [24] and Madison [25] conventions is given by

$$A_y = \frac{\sigma_L - \sigma_R}{\sigma_L + \sigma_R} \tag{6}$$

where σ_L and σ_R are the double differential cross sections for the emission of the helions to the left and right of the incident particle beam respectively. Thus the multistep expression for the analyzing power becomes

$$A_{multistep} = \frac{A_1 \left(\frac{d^2\sigma}{d\Omega dE}\right)^{\text{one-step}} + A_2 \left(\frac{d^2\sigma}{d\Omega dE}\right)^{\text{two-step}} + \ldots}{\left(\frac{d^2\sigma}{d\Omega dE}\right)^{\text{one-step}} + \left(\frac{d^2\sigma}{d\Omega dE}\right)^{\text{two-step}} + \ldots} \quad , \tag{7}$$

with A_i , $i = 1, 2, \ldots$ referring to analyzing powers for the successive multisteps.

4 Results

Double differential cross section angular distributions for the ($\vec{p}$,^{3}He) reaction on ^{59}Co and ^{93}Nb at incident proton energies E_p of 100 and 130 MeV, and at various outgoing ^{3}He energies, are shown in Figure 1. According to the phenomenological systematics of Kalbach [26] the distributions are given by

$$\frac{d^2\sigma}{d\Omega dE} = A \frac{a}{\sinh a} \, e^{a \cos\theta} \tag{8}$$

as a function of scattering angle θ and a normalisation constant A, which depends on emission energy. The slope parameter a is to a good approximation only a function of the ratio of emission energy to incident energy. The good agreement between the phenomenological predictions and the experimental distributions provides some guidance as to what relationships should exist between the data sets at different incident and emission energies.

In Figure 2 results of the statistical multistep direct deuteron pickup theory are compared with differential cross section angular distributions at an incident energy of 130 MeV for various emission energies. For both target nuclei we find a rapid drop-off of the first step as the emission energy decreases, as found in previous work [2, 17]. The theory gives a good reproduction of the experimental distributions. The corresponding analyzing power distributions are shown in Figure 3, and this demonstrates how the various steps conspire to influence the shape of the observed angular distributions at different emission energies. Again the theoretical distributions are in reasonable agreement with the experimental analyzing power distributions, thus showing that the theory describes both observables in a consistent way. The trend of the analyzing power towards zero as more steps contribute to the value is clear.

Finally, in Figures 4 and 5 the analyzing power results are shown for ^{59}Co and ^{93}Nb at a fixed excitation energy, and an emission energy that represents roughly 80% of the incident energy, respectively. The latter comparison is motivated by the Kalbach systematics. The results are qualitatively similar for the two representative examples displayed.

Clearly the multistep theory describes the experimental cross section and analyzing power distributions well at all three incident energies between 100 and 160

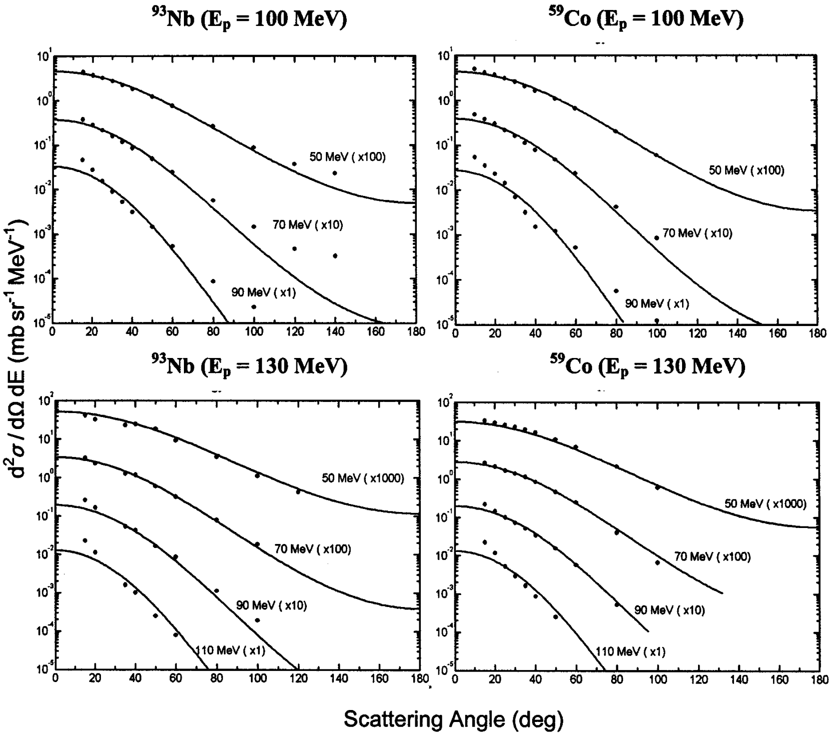

Figure **1.** Differential cross section distributions for the ($\vec{p}$,^{3}He) reaction on ^{59}Co and ^{93}Nb at two incident energies for various outgoing energies. The lines are predictions of the phenomenology of Kalbach [26]. The experimental distributions at an incident energy of 100 MeV are from Cowley *et al.* [2] and those at 130 MeV from the present work.

MeV. Furthermore, the inputs to the calculations are those that are known to provide good fits to elastic scattering data [16,19] that are not directly related to the inclusive ($\vec{p}$,^{3}He) reaction of this work, with the imaginary part of the ^{3}He optical potential being the only ingredient that we vary to best-fit the data. In this regard it should be noted that this potential varies systematically with incident energy, as shown in Figure 6 where the volume integral of the imaginary ^{3}He optical potential is shown as a function of incident energy. Although the incident proton energy, and its wave function should be unrelated to the ^{3}He potential to first order, the observed relationship is reasonable if one keeps in mind that we determine the latter by requiring a good fit to data at low excitation energy, in other words we use the range where the one-step mechanism dominates. Thus we implicitly also emphasise a value of the ^{3}He energy which varies with incident energy. Clearly the energy variation of the ^{3}He imaginary optical potential implies that this needs to be taken into account as the emission energy varies for a specific incident energy. For lack of theoretical guidance this has been ignored in this work.

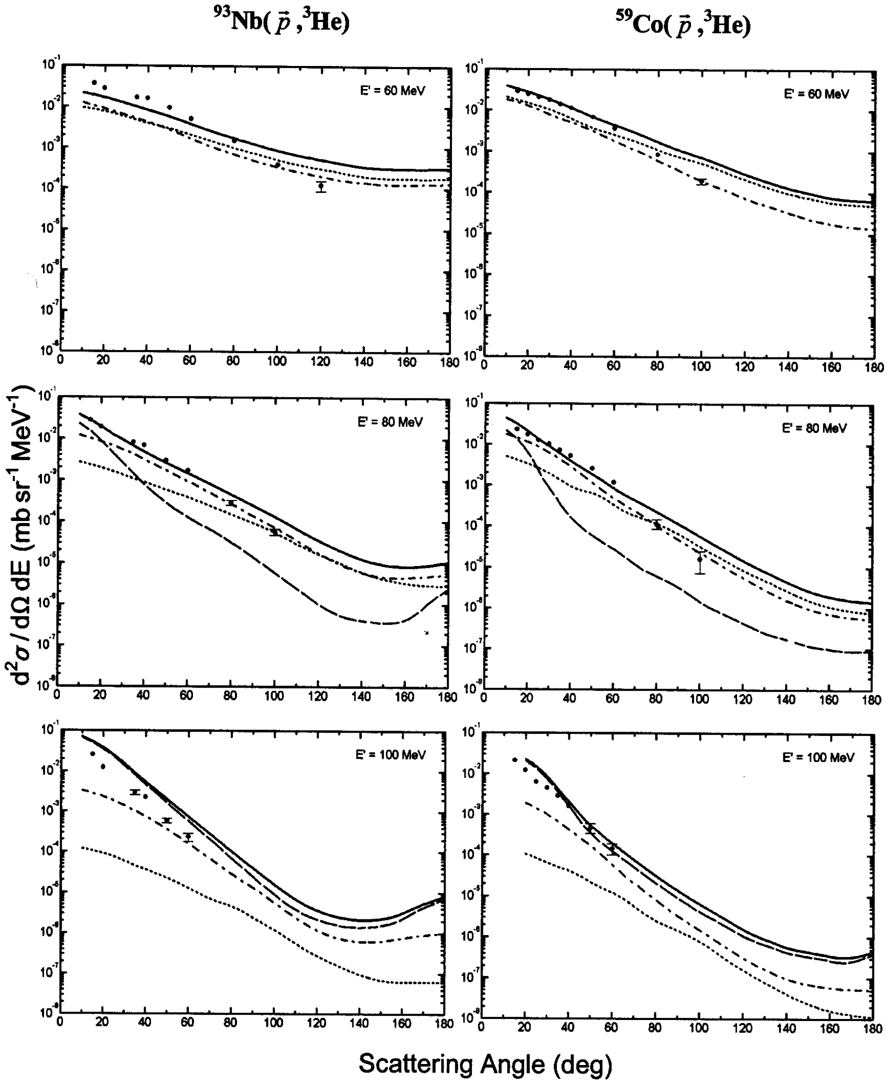

Figure **2.** Experimental laboratory double differential cross sections as a function of scattering angle θ for ^{93}Nb($\vec{p}$,^{3}He) and ^{59}Co($\vec{p}$,^{3}He) at an incident energy of 130 MeV and various outgoing energies E' (statistical uncertainties are displayed where they exceed the symbol size), compared with calculations for one step (— — —) two step (— · — · —) and three step (· · · · ·) contributions. The sums of the contributions are given by continuous curves.

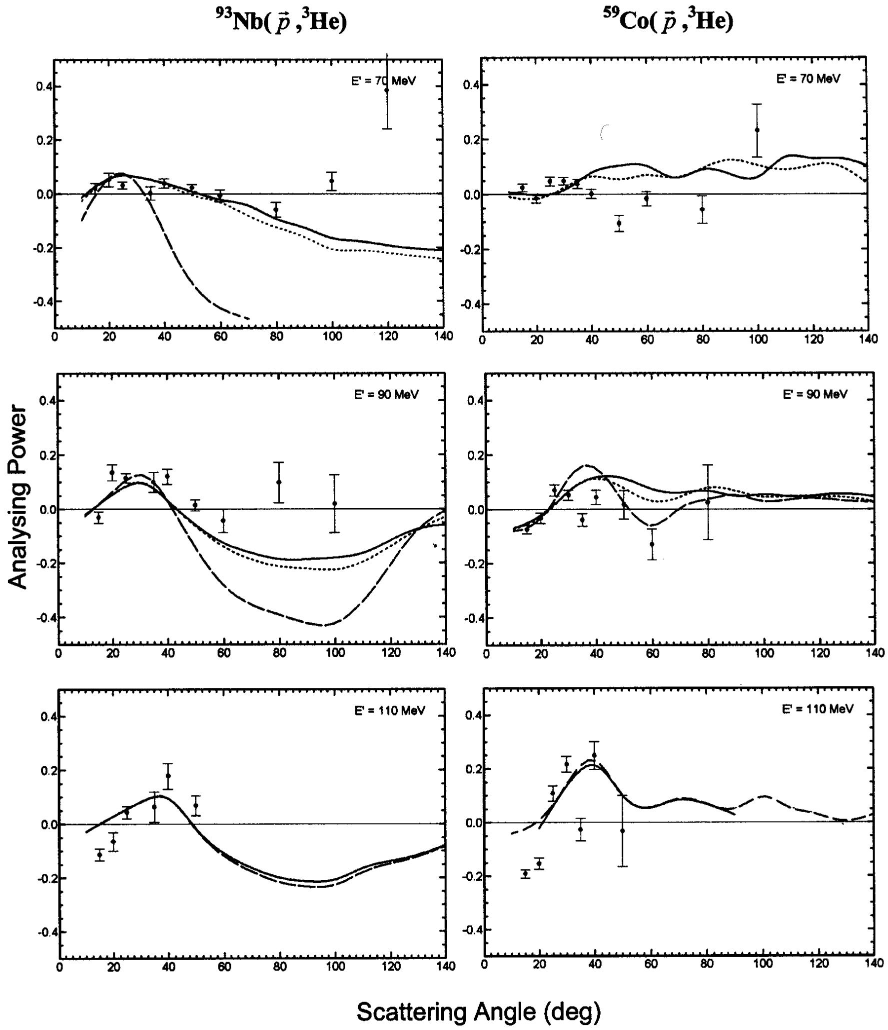

Figure **3.** Experimental analyzing powers as a function of scattering angle θ for ^{93}Nb($\vec{p}$,^{3}He) and ^{59}Co($\vec{p}$,^{3}He) at an incident energy of 130 MeV and various outgoing energies E' (statistical error bars are shown where they exceed the symbol size) compared with calculations for one step (— — —) and one + two step (· · · · ·) contributions. The sums of the contributions from three steps are given by continuous curves.

5 Summary and Conclusions

The present investigation of the differential cross sections and analyzing powers of the ($\vec{p}$,^{3}He) reaction on ^{59}Co and ^{93}Nb to the continuum has extended the previous analyses [2] at lower incident energy. As was found previously, the analyzing powers prove to be a sensitive measure of the contributions of the various one-step and

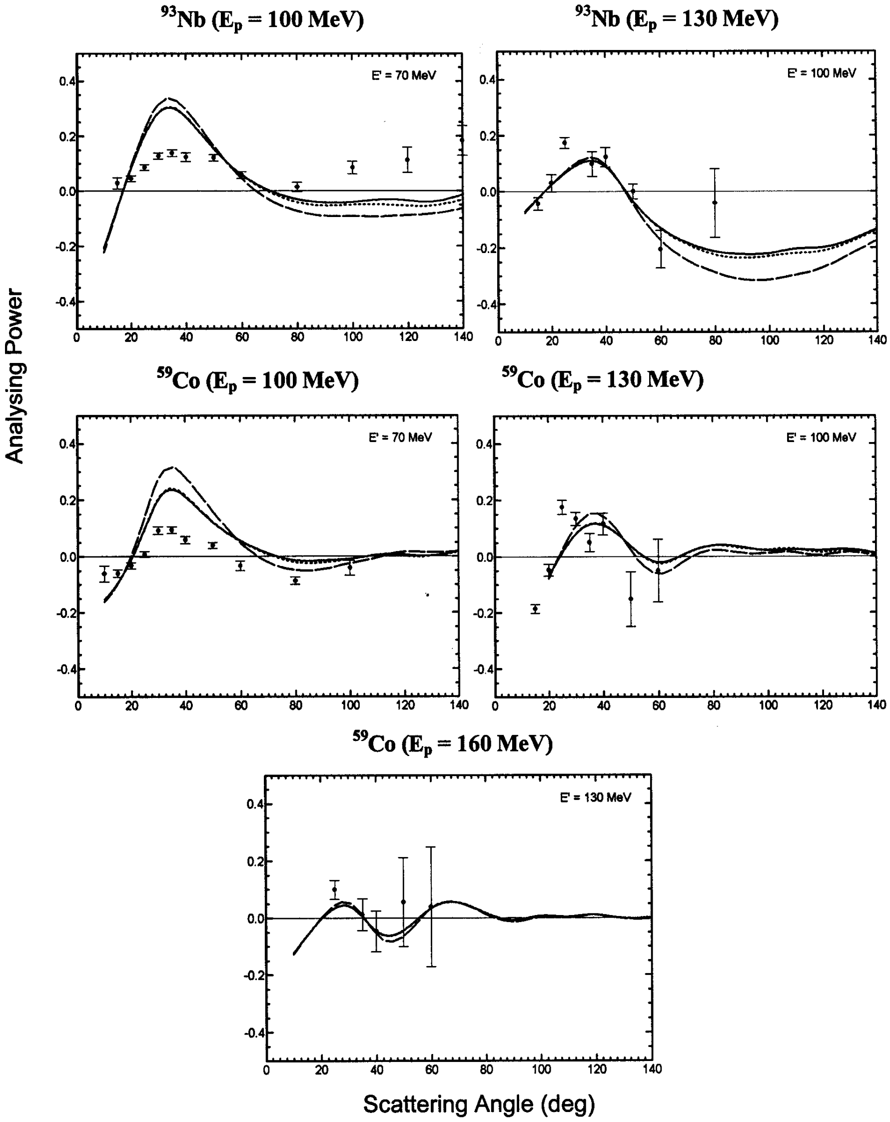

Figure **4.** Experimental analyzing powers as a function of scattering angle θ for ^{93}Nb($\vec{p}$,^{3}He) and ^{59}Co($\vec{p}$,^{3}He) at incident energies of 100, 130 and 160 MeV at outgoing energies E' of 30 MeV lower than the respective incident energies (statistical error bars are shown where they exceed the symbol size) compared with calculations for one step (— — —) and one + two step (· · · · ·) contributions. The sums of the contributions from three steps are given by continuous curves.

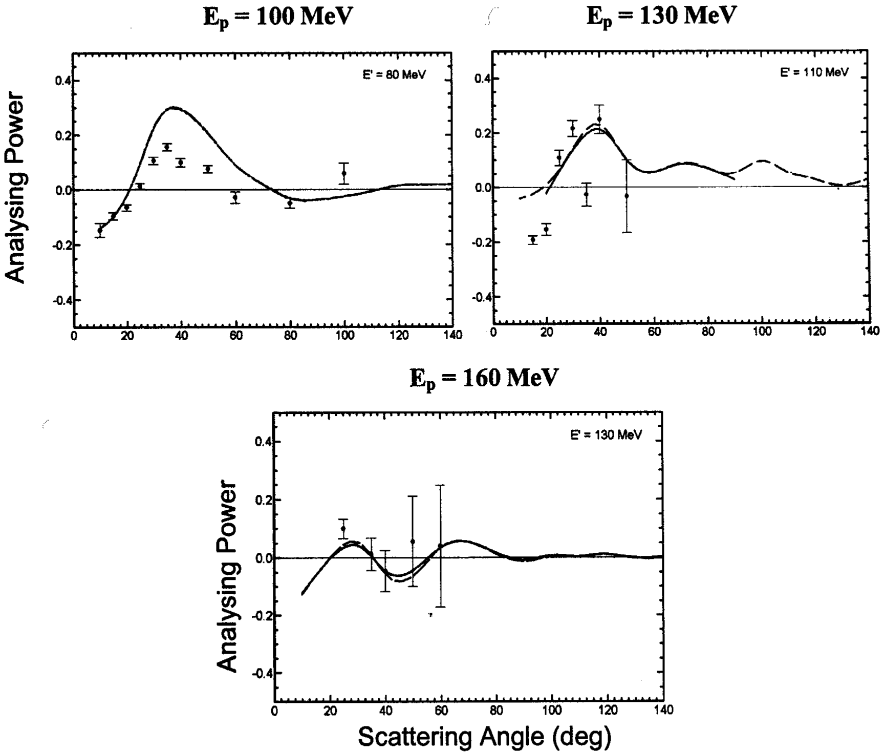

Figure **5.** Experimental analyzing powers as a function of scattering angle θ for ^{59}Co($\vec{p}$,^{3}He) at incident energies of 100, 130, and 160 MeV and at outgoing energies E' corresponding to approximately 80% of the incident energy (statistical error bars are shown where they exceed the symbol size) compared with calculations for one step (— — —) and one + two step (· · · · ·) contributions. The sums of the contributions from three steps are given by continuous curves.

multistep processes. Also, the re-analysis of the 100 MeV data gives essentially the same results as found previously [2], which proves that the calculations are not very sensitive to the exact details or implementation of the theory. This shows that the interpretation remains consistent as the incident energy is increased. We find, as expected physically, that the analyzing power decreases as two-step and three-step processes become dominant. Results from the two target species are qualitatively similar, which suggests that these results are characteristic of nuclei in general.

The results of the theoretical multistep pickup calculations are in reasonable agreement with the experimental cross section and analyzing power angular distributions. Thus the theory appears to contain the basic physics of the reaction mechanism. Nevertheless, one would have preferred to find improved overall agreement between theory and experiment, but it is difficult to see how the calculation can be meaningfully improved. The lack of an accurate knowledge of the ^{3}He optical potentials is the main deficiency of the present theoretical predictions. Clearly a better

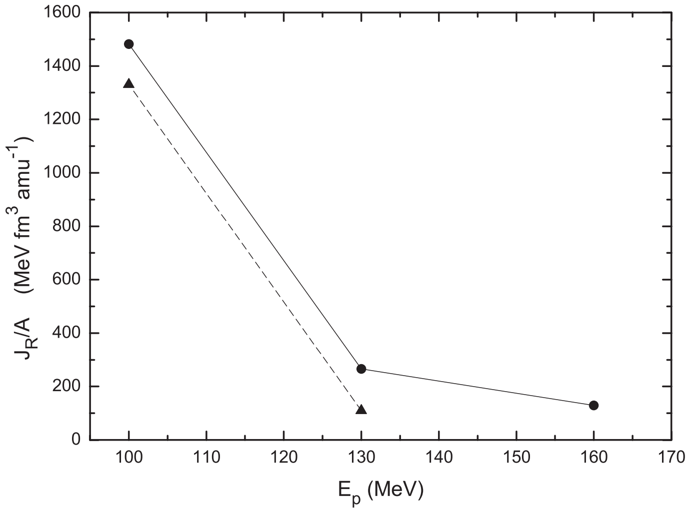

Figure **6.** Volume integral of the imaginary potential for ^{3}He extracted at incident proton energies of 100, 130 and 160 MeV for target nuclei ^{59}Co (circles) and ^{93}Nb (triangles). Note that the results for ^{93}Nb have been multiplied by a factor of 5 for clarity of display.

understanding of these optical potentials would allow the meaningful introduction of further refinements to the theory. Other possible reaction mechanisms, such as sequential pickup, should also be considered, but this is beyond the scope of the present work.

Acknowledgments

We thank M. Katsuma and Y. Sakuragi for kindly providing their double folding code MOPHE3, and P. Demetriou for numerical values of (p, p') and (p, p', p'') cross sections. Use of nuclear density distributions calculated by M.V. Stoitsov is gratefully acknowledged. S.S.D. thanks the Royal Society and the Bulgarian Science Foundation for financial support (Contracts Φ–1416 and Φ–1501) and the Nuclear and Astrophysics Laboratory of Oxford University for its hospitality. A.A.C. thanks the Nuclear and Astrophysics Laboratory of Oxford University for its hospitality and the Oppenheimer Fund for financial support during the period when a crucial part of this research was performed. P.E.H. also gratefully acknowledges support from the Oppenheimer Fund. This work was also funded by the South African National Research Foundation under Grant Number GUN2053773.

References

1. R. Bonetti, F. Crespi, and K.-I. Kubo, *Nucl. Phys. A* **499**, 381 (1989).
2. A. A. Cowley, G. F. Steyn, S. S. Dimitrova, P. E. Hodgson, G. J. Arendse, S. V. Förtsch, G. C. Hillhouse, J. J. Lawrie, R. Neveling, W. A. Richter, J. A. Stander, and S. M. Wyngaardt, *Phys. Rev. C* **62**, 064605 (2000).
3. E. Renshaw, S. J. Yennello, K. Kwiatkowski, R. Planeta, L. W. Woo, and V. E. Viola, *Phys. Rev. C* **44**, 2618 (1991).
4. J. V. Pilcher, A. A. Cowley, D. M. Whittal, and J. J. Lawrie, *Phys. Rev. C* **40**, 1937 (1989).
5. D. M. Whittal, A. A. Cowley, J. V. Pilcher, F. D. Smit, S. V. Förtsch, and J. J. Lawrie, *Phys. Rev. C* **42**, 309 (1990).
6. H. Feshbach, A. Kerman and S. Koonin, *Ann. Phys.* **125**, 429 (1980).
7. R. Bonetti, L. Colli Milazzo, I. Doda and P. E. Hodgson, *Phys. Rev. C* **26**, 2417 (1982).
8. J. N. Bishop, L. R. Medsker, and H. T. Fortune, *Phys. Rev. C* **20**, 1221 (1979).
9. J. S. Sens and R. J. de Meijer, *Nucl. Phys. A* **407**, 45 (1983).
10. E. Gadioli and E. Gadioli Erba, *J. Phys. G* **8**, 83 (1982).
11. H. Nann, W. Benenson, W. A. Lanford, and B. H. Wildenthal, *Phys. Rev. C* **10**, 1001 (1974).
12. P. D. Kunz and E. Rost in *Computational Nuclear Physics*, edited by K. Langanke *et al*. Springer-Verlag, Berlin, Vol. 2, Chap. 5 (1993).
13. R. J. de Meijer, L. W. Put, and J. C. Vermeulen, *Phys. Lett. B* **107**, 14 (1981).
14. R. J. de Meijer, L. W. Put, J. J. Akkermans, J. C. Vermeulen, and C. R. Bingham, *Nucl. Phys. A* **386**, 200 (1982).
15. D. G. Madland (1988) in *Proceedings of Specialists' Meeting on Pre-Equilibrium Reactions*, Semmering, Austria, edited by B. Strohmaier OECD, Paris, p. 103; International Atomic Energy Report No. IAEA-TECDOC-483, p. 80 (1980).
16. P. Schwandt, H. O. Meyer, W. W. Jacobs, A. D. Bacher, S. E. Vigdor, M. D. Kaitchuck, and T. R. Donoghue, *Phys. Rev. C* **26**, 55 (1982).
17. A. A. Cowley, G. J. Arendse, G. F. Steyn, J. A. Stander, W. A. Richter, S. S. Dimitrova, P. Demetriou, and P. E. Hodgson, *Phys. Rev. C* **55**, 1843 (1997).
18. G. R. Satchler and W. G. Love, *Phys. Reports* **55**, 183 (1979).
19. J. Cook, *Nucl. Phys. A* **465**, 207 (1987).
20. A. M. Kobos, B. A. Brown, P. E. Hodgson, G. R. Satchler, and A. Budzanowski, *Nucl. Phys. A* **384**, 65 (1982).
21. M. Katsuma and Y. Sakuragi (2000) private communication.
22. A. A. Cowley, G. J. Arendse, J. W. Koen, W. A. Richter, J. A. Stander, G. F. Steyn, P. Demetriou, P. E. Hodgson, and Y. Watanabe, *Phys. Rev. C* **54**, 778 (1996).
23. W. A. Richter, A. A. Cowley, G. C. Hillhouse, J. A. Stander, J. W. Koen, S. W. Steyn, R. Lindsay, R. E. Julies, J. J. Lawrie, J. V. Pilcher, and P. E. Hodgson, *Phys. Rev. C* **49**, 1001 (1994).
24. P. Huber and K. P. Meyer in *Proceedings of the First International Symposium on Polarization Phenomena of Nucleons*, Basel, Switzerland (1960).
25. H.H. Barschall and W Haeberli in *Proceedings of the Third International Symposium on Polarization Phenomena in Nuclear Reactions*, Madison, Wisconsin, USA (1971).
26. C. Kalbach, *Phys. Rev. C* **37**, 2350 (1988).